THE JOURNAL OF BIOLOGICAL CHEMISTRY VOL. 286, NO. 27, pp. 24385–24393, July 8, 2011

The Cell Adhesion Molecule Neurofascin Stabilizes Axo-axonic GABAergic Terminals at the Axon Initial Segment*[S]

Received for publication, December 14, 2010, and in revised form, May 3, 2011 Published, JBC Papers in Press, May 16, 2011, DOI 10.1074/jbc.M110.212191

Martin Kriebel[‡1], Jennifer Metzger[‡1], Sabine Trinks[‡], Deepti Chugh[‡§2], Robert J. Harvey[¶], Kirsten Harvey[¶], and Hansjürgen Volkmer[‡3]

From the [‡]Naturwissenschaftliches und Medizinisches Institut an der Universität Tübingen, 72770 Reutlingen, Germany, the [¶]Department of Pharmacology, the School of Pharmacy, University of London, London WC1N 1AX, United Kingdom, and the [§]Graduate School of Cellular and Molecular Neuroscience, Universität Tübingen, D-72074 Tübingen, Germany

Cell adhesion molecules regulate synapse formation and maintenance via transsynaptic contact stabilization involving both extracellular interactions and intracellular postsynaptic scaffold assembly. The cell adhesion molecule neurofascin is localized at the axon initial segment of granular cells in rat dentate gyrus, which is mainly targeted by chandelier cells. Lentiviral shRNA-mediated knockdown of neurofascin in adult rat brain indicates that neurofascin regulates the number and size of postsynaptic gephyrin scaffolds, the number of $GABA_A$ receptor clusters as well as presynaptic glutamate decarboxylase-positive terminals at the axon initial segment. By contrast, overexpression of neurofascin in hippocampal neurons increases gephyrin cluster size presumably via stimulation of fibroblast growth factor receptor 1 signaling pathways.

Signal transduction in the nervous system relies on an elaborate balance between excitatory and inhibitory synaptic transmission. Formation and stabilization of both types of synapses involve the recruitment of cell surface molecules and intracellular scaffold components to postsynaptic sites (1). Cell adhesion molecules are thought to stabilize synaptic contacts as exemplified by postsynaptic neuroligin interactions with presynaptic neurexins (2). For example, neuroligin 2 is involved in the stabilization of dendritic (3) and perisomatic inhibitory synapses (4). However, little is known about the stabilization of axo-axonic GABAergic synapses targeting the axon initial segment (AIS).[4] The AIS of cortical and hippocampal neurons is a specialized region that receives input mainly from axo-axonic GABAergic interneurons (5). Chandelier cells represent the prominent class of interneurons providing presynaptic terminals to the AIS (6). Chandelier cells are parvalbumin-positive interneurons that extend rows of presynaptic boutons for axo-axonic innervation along the AIS. Chandelier terminals are strategically located at the site of action potential initiation and are therefore suspected to regulate neuronal signal propagation, the precise mechanism being under dispute (7). Interestingly, reduced GABAergic innervation at the AIS of cortical layer 2/3 pyramidal neurons appears to be specific to the disease process of schizophrenia (8).

The AIS represents a special compartment in neurons that is characterized by the presence of specific proteins (9) including ankyrin G, βIV spectrin, β1 subunits of sodium channels, and neuronal cell adhesion molecules neurofascin and NrCAM (10–12). Neurofascin is expressed in different major isoforms generated by alternative splicing, *e.g.* NF155, NF166, and NF186 (13). Although NF155 is found in glia, the neuronal NF186 isoform is tethered to the ankyrin-based cytoskeleton at AIS where it may serve as a organizer of the perineuronal net (14) and contributes to sodium channel clustering at the nodes of Ranvier (15, 16). By contrast, NF166 is implicated in the induction of neurite outgrowth via FGFR1 signaling (17) and may be involved in the induction of gephyrin clusters in immature hippocampal neurons devoid of differentiated AIS (18). However, the role of neurofascin in the maintenance of inhibitory input in the adult brain is still unclear because of early mortality of neurofascin knock-out mice (16). Here, we apply *in vivo* studies in the adult brain in combination with *in vitro* systems to study the function of neurofascin in the organization of gephyrin clusters and the stabilization of presynaptic axo-axonic input at the AIS.

EXPERIMENTAL PROCEDURES

Lentiviral Vector Construction and Lentiviral Production—A CamKII/EGFP/woodchuck hepatitis virus posttranscriptional regulatory element-expression cassette from L22 FCK-1.3 (Pavel Osten) was introduced into pLenti6/BLOCK-iT™-DEST (Invitrogen) to yield pLenti/CEW. Subsequently, control

* This work was supported in part by European Union Grant LSHM-CT-2005-512012 and Bundesministerium für Bildung und Forschung Grant 0315512 (to H. V.) and Medical Research Council Grants G0501258 and G0800498 (to K. H. and R. J. H.).

[S] The on-line version of this article (available at http://www.jbc.org) contains supplemental text and a figure.

[1] Both authors contributed equally to this work.

[2] Supported by a scholarship from the Hertie-Institute for Clinical Brain Research.

[3] To whom correspondence should be addressed: NMI an der Universität Tübingen, Markwiesenstr. 55, 72770 Reutlingen, Germany. Tel.: 49-7121-5153044; Fax: 49-7121-5153016; E-mail: volkmer@nmi.de.

[4] The abbreviations used are: AIS, axon initial segment; CAM, cell adhesion molecule; CamKII, Ca^{2+}/calmodulin-dependent protein kinase II; CB, collybistin; DIV, days *in vitro*; dnFGFR1, dominant negative FGF receptor 1; EGFP, enhanced green fluorescent protein; FGFR1, fibroblast growth factor receptor 1; FNIII, fibronectin type III; GABA, γ-aminobutyric acid; $GABA_AR$, GABA type A receptor; GAD65, glutamate decarboxylase; GAT-1, GABA transporter 1; NCAM, neural cell adhesion molecule; NF, neurofascin; VGSC, voltage-gated sodium channel.

(shCTR) and neurofascin-specific (shNF252/1504) shRNA sequences were integrated via Gateway® recombination (Virapower™ Lentiviral Expression System; Invitrogen), and lentiviral particles were produced according to the manufacturer's protocols (viral titers approximately 5×10^7 transducing units/ml).

Animals, Stereotactic Surgery, Transcardial Perfusion—Adult female Sprague-Dawley rats (250 g at time point of surgery; Charles River Laboratories) were kept in compliance with the European Union recommendations for the care and use of laboratory animals and as approved by the responsible regional council. For stereotactic injection of lentiviral suspension, animals were deeply anesthetized by injection of ketamine/xylazine (100 mg/kg and 10 mg/kg, respectively). Bilateral injections of 4 μl of lentiviral suspensions into the dorsal dentate gyrus (AP: −2.9 mm, ML: ± 2.5 mm, DV: −4.3 mm; all coordinates relative to Bregma) were conducted using a Lab Standard™ Stereotaxic Instrument (Stoelting Co., Wood Dale, IL) connected to a 701 RN Hamilton syringe (10 μl, 30 gauge, pst 4; CS-Chromatographie Service, Langerwehe, Germany). Injection speed was set to 0.2 μl/min. For fixation of brain tissue, animals were deeply anesthetized as described above and perfused transcardially with 200 ml of 1 × PBS followed by 500 ml of 4% paraformaldehyde/PBS.

Cell Culture and Transfection—Culture and transient transfection of HeLa cells and primary neurons were performed as described previously (18, 19). Primary hippocampal neurons were cultured at high density (2×10^5 cells/cm^2). Transfection was performed at 10 days *in vitro* (DIV), and cultures were processed for imaging at 17 DIV. Plasmids used were: pEGFP-C2/gephyrin, pRK5myc/collybistin II ($CB2_{SH3-}$), pcDNA3.1myc-his/FGFR1 and pEGFP-N1/FGFR1-DN (17), expression vectors for chick neurofascin-166, −166ED, −166CD, and −186 (18), pCMV/NCAM (full-length NCAM180 cDNA cloned into pEGFP-N1 (Clontech) via XhoI and NotI restriction sites, pCMV/$GABA_A$R-α2 and pCMV/$GABA_A$R-β3 (full-length subunits cloned into pEGFP-N1 via SacII-NotI restriction sites), pEGFP-N1/$GABA_A$R-γ2, pcDNA3.1-L1 (kindly provided by Vance Lemmon). Equal amounts of plasmid DNA were transfected in all cases. Inhibitors were dissolved in dimethyl sulfoxide and added to the cell culture medium at the start of transfection to a final concentration of 20 μM for FGFR1 inhibitor SU5402, 10 μM for MEK inhibitor U0126, and 10 μM for PI3K inhibitor LY294002.

Immunohistochemistry—For immunohistochemistry the following primary antibodies were used: anti-gephyrin (mAb7a, 1:100; Synaptic Systems, Göttingen, Germany), mAb anti-voltage-gated sodium channel (VGSC) (1:100; Sigma-Aldrich), polyclonal antibodies anti-GAD65 (1:1000; Millipore), anti-GAT1 (1:500; Millipore), anti-neurofascin (17), anti-VGSC (1:100; Sigma-Aldrich), and anti-NCAM (1:100, kind gift from V. Berezin and E. Bock). Perfusion-fixed brains were washed in PBS and cut into 100-μm slices using a vibrating microtome (Vibroslice 752 M; Cambden Instruments, Loughborough, UK). After permeabilization (0.6% Triton X-100), slices were blocked by 1 × BMB blocking reagent/PBS (Roche Applied Science) for 1 h at room temperature. Further processing of brain slices and immunocytochemical staining were performed as described (18, 19). Specimens were mounted on microscopic slides using Dako Fluorescent Mounting medium (Dako GmbH, Hamburg, Germany).

Image Acquisition and Statistical Analysis—Confocal fluorescence images were acquired at 23 °C using a Zeiss LSM510 Meta confocal microscope equipped with a 63× Plan-Apochromat oil immersion objective (NA 1.4; Carl Zeiss AG, Oberkochen, Germany). Z-stack images of hippocampal slices were recorded, processed and analyzed as detailed in the supplemental text (Imaris software package, Bitplane AG, Zurich, Switzerland). HeLa cells were fixed and analyzed 24 h after transient transfection. For quantitative analysis of gephyrin cluster size, images of 20–40 cells were taken using the Zeiss LSM510 Meta confocal microscope equipped with a 63× Plan-Apochromat oil immersion objective. The images were analyzed using Imaris software package. The areas of individual gephyrin clusters were determined and used to calculate the mean size of individual gephyrin clusters. At least three independent transfections or animals were used for each experiment shown.

RNA Preparation and RT-PCR Analysis—Total RNA from rat brain tissue (Sprague-Dawley) was prepared using RNA-STAT60 reagent according to the manufacturer's guidelines (AMS Biotechnology, Milton, UK). Total RNA from staged hippocampal neurons was isolated using the RNAqueous®-4PCR Kit (Ambion, Austin, TX). cDNA synthesis was performed with the High Capacity RNA-to-cDNA Kit (Applied Biosystems). SYBR Green quantitative RT-PCR to amplify neurofascin-specific sequences was carried out on the 7500 Fast Real-Time PCR System (Applied Biosystems) using the following primer sets: NF186-F (TGGAAGCACAATTTCAGGCC) and NF186-R (CTGATGCCCTCGTTGTCCCG), NF166-F (GTACCTACCACCGTCGCCA) and NF166-R (TGGTGTAAGCGGTTTCGTGA), GAPDH-F (TGCACCACCAACTGCTTAGC) and GAPDH-R (GGCATGGACTGTGGTCATGAG).

RESULTS

Neurofascin Is Expressed on Axon Initial Segments of Granular Cells in the Dentate Gyrus—Hippocampal slices from rat brain were immunostained for neurofascin, VGSC as a marker for the AIS, as well as GABA transporter 1 (GAT-1), GAD65, and gephyrin as presynaptic and postsynaptic markers of GABAergic synapses. Different neurofascin isoforms are expressed both in neurons and glial cells. For unambiguous allocation of neuronal neurofascin, single granular cells were labeled via lentiviral expression of EGFP driven by the Ca^{2+}/calmodulin-dependent protein kinase II (CamKII) promoter (Fig. 1*A*; for details see the supplemental figure). Rendered images of EGFP-labeled granular cells (Fig. 1*A′*) were used to identify VGSC and neurofascin signals as shown in Fig. 1*A″* and 1*A‴*. VGSC colocalizes with neurofascin, indicating that neurofascin is localized at the AIS of granular neurons in the dentate gyrus as previously observed in dissociated hippocampal neurons (18). Pan-VGSC antibodies were used recognizing all known vertebrate VGSCs. Previous reports have documented that axo-axonic interneurons target the AIS of hippocampal pyramidal and granular cells (20). At the AIS, presynaptic terminals of axo-axonic, parvalbumin-positive chandelier neurons can be stained for GAT-1 (6). As shown in Fig. 1, *B–D*,

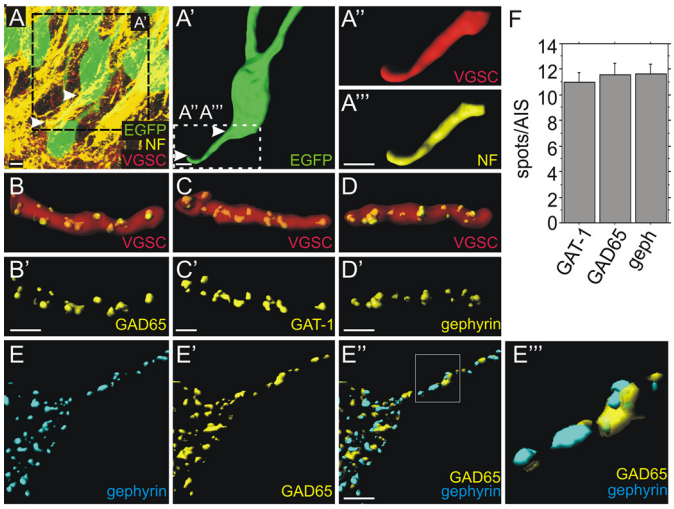

FIGURE 1. **Localization of neurofascin and number of synaptic terminals at the AIS of hippocampal granule cells.** *A*, confocal image of adult dentate gyrus granular cells labeled by lentivirally expressed EGFP (*green*). *Arrowheads* indicate the AIS. *A′*, rendering of the EGFP signal depicting a single granular cell (*green*) corresponding to the *boxed* region in *A*. *A″* and *A‴*, further magnification of the *inset* in *A′* showing VGSC (*red*) or neurofascin (*yellow*) staining at the AIS corresponding to the *boxed* region in *A′*. *B* and *C*, GAD65- and GAT-1-positive presynaptic terminals (*yellow*) visualized on VGSC-stained AIS of uninfected granular cells (*red*). *D*, postsynaptic gephyrin spots (*yellow*) localized on VGSC-stained AIS of uninfected granular cells (*red*). *B′–D′*, same images as in *B–D* with the VGSC signals omitted. *Scale bars*: 5 μm. *E–E‴*, localization of opposed postsynaptic gephyrin (*E*) and presynaptic GAD65 (*E′*) clusters (merged in *E″*) on a granule cell AIS *in vivo*. An enlargement of the *rectangle* in *E″* is shown in *E‴*. Brightness and contrast were slightly adjusted in *E‴* to visualize structures of low pixel intensity. *F*, quantification of GAD65- and GAT-1-positive presynaptic terminals as well as gephyrin-positive postsynaptic sites at the AIS of uninfected cells (not significant, ANOVA; $n = 20$ for all groups, *error bars* represent S.E.).

GAT-1-, GAD65-, and gephyrin-positive punctae were found at the VGSC-positive AIS in accordance with previous findings (21). Likewise, 11–12 puncta for GAD65, GAT-1, and gephyrin per AIS were identified (Fig. 1*F*), suggesting that components of synapses formed by chandelier cells were stained. As shown in Fig. 1, *E–E‴*, all gephyrin-positive clusters were opposed to a presynaptic GAD65 signal on the granule cell AIS. Hence, neurofascin is located on the AIS of granular cells in the dentate gyrus targeted by GABAergic presynaptic terminals.

Neurofascin Is Required for the Stabilization of GABAergic Synapses—To analyze a possible role of neurofascin in synapse stabilization in the adult dentate gyrus, neurofascin expression was inhibited by lentiviral shRNA expression after stereotactic injection in rat brain. Specificity, the efficacy and absence of off-target effects have been assessed in a previous report (18). Lentiviral vectors for the expression of an ineffective control shRNA (shCTR), neurofascin-specific shRNAs (shNF252 and shNF1504) together with CamKII promoter-driven EGFP were injected into the rat dentate gyrus. After 14 days, hippocampal slices were stained for the presynaptic marker GAD65 and postsynaptic gephyrin as well as VGSC as an AIS marker. Infected granular cells were identified via EGFP expression (Fig. 1). The number of GAD65, gephyrin, or $GABA_A$ receptor subunit β2/3 punctae did not significantly differ on the AIS of shCTR-infected and uninfected neurons, indicating that lentiviral infection alone did not interfere with synapse stability (Fig. 2, *M*, *Q*, and *U*). By contrast, infected neurons expressing shNF252 displayed <50% of GAD65, gephyrin, or $GABA_A$R subunit β2/3 punctae at the AIS compared with controls (Fig. 2, *J*, *N*, and *R*). The effects observed are unlikely to be due to off-target effects, because an independent neurofascin-specific shRNA vector (shNF1504) was equally effective (Fig. 2*V*). Crucially, inspection of GAD65, gephyrin, or $GABA_A$R subunit β2/3 clusters on somata or dendrites did not reveal significant differences in puncta number (Fig. 2, *K*, *L*, *O*, *P*, *S*, and *T*). Hence, the observed reductions for GABAergic markers were specific for the AIS, reflecting the specificity of neurofascin expression in this structure.

We also examined the mean gephyrin cluster volume and the total gephyrin cluster volume per AIS after neurofascin knockdown. As expected, the total cluster volume per AIS was significantly decreased, in accordance with the observed reduction in gephyrin cluster number (Fig. 2*X*). Interestingly, knockdown of neurofascin also decreased the mean gephyrin cluster volume (Fig. 2*W*). Thus, as well as controlling gephyrin cluster number, neurofascin may also be involved in the control of gephyrin cluster size.

VGSC staining was used to identify the AIS of infected and uninfected granular cells. Because neurofascin is thought to regulate the surface expression of sodium channels (22), we quantified immunohistological staining for VGSC after knockdown of neurofascin *in vivo* (Fig. 2*Y*). However, we did not observe any differences in VGSC staining between control and shNF252-infected neurons at the AIS. This finding is consistent with a recent report that neurofascin knockdown in hippocampal neurons does not interfere with VGSC or ankyrin G localization at the AIS (23). Consequently, lentiviral knockdown of neurofascin does not impair the expression of the AIS marker VGSC *in vivo*.

Neurofascin Overexpression Modulates Gephyrin Clustering in Hippocampal Neurons—Two functionally distinct neuronal neurofascin isoforms are found in brain, mainly differing in the expression of the fifth FNIII-like repeat which is absent in NF166 ($NF_{-5.FNIII}$) and present in NF186 ($NF_{+5.FNIII}$) (19, 24). Analysis of the expression of neurofascin in rat brain revealed (Fig. 3*H*) that $NF_{-5.FNIII}$ is expressed in a 7-fold and 37-fold excess over $NF_{+5.FNIII}$ at embryonic day 17 and postnatal day 3. By contrast, the ratio was reversed in the adult brain. Here, $NF_{+5.FNIII}$ was expressed in a 33-fold excess over $NF_{-5.FNIII}$. This indicates that predominant $NF_{+5.FNIII}$ expression is a hallmark of mature neurons *in vivo*. Inspection of cultured hippocampal neurons revealed that the ratio of $NF_{-5.FNIII}$ to $NF_{+5.FNIII}$ continuously declined from 18.3 (5 DIV) to 0.7 (39 DIV) (Fig. 3*G*). Hence, cultured neurons differ from adult brain in the increased expression of $NF_{-5.FNIII}$.

Next, the impact of neurofascin NF166 ($NF_{-5.FNIII}$) was examined after overexpression in primary hippocampal neurons. Although the number of endogenous gephyrin clusters remained unaffected, NF166 decreased the average size of individual gephyrin clusters (Fig. 3, *A* and *B*). On the other hand, cotransfection of neurofascin NF166 and EGFP-gephyrin increased cluster size, indicating that endogenous and overexpressed gephyrin were regulated differently (Figs. 3*C* and 4, *A* and *B*). To address possible overexpression artifacts, we included further controls to analyze clustering of exogenous

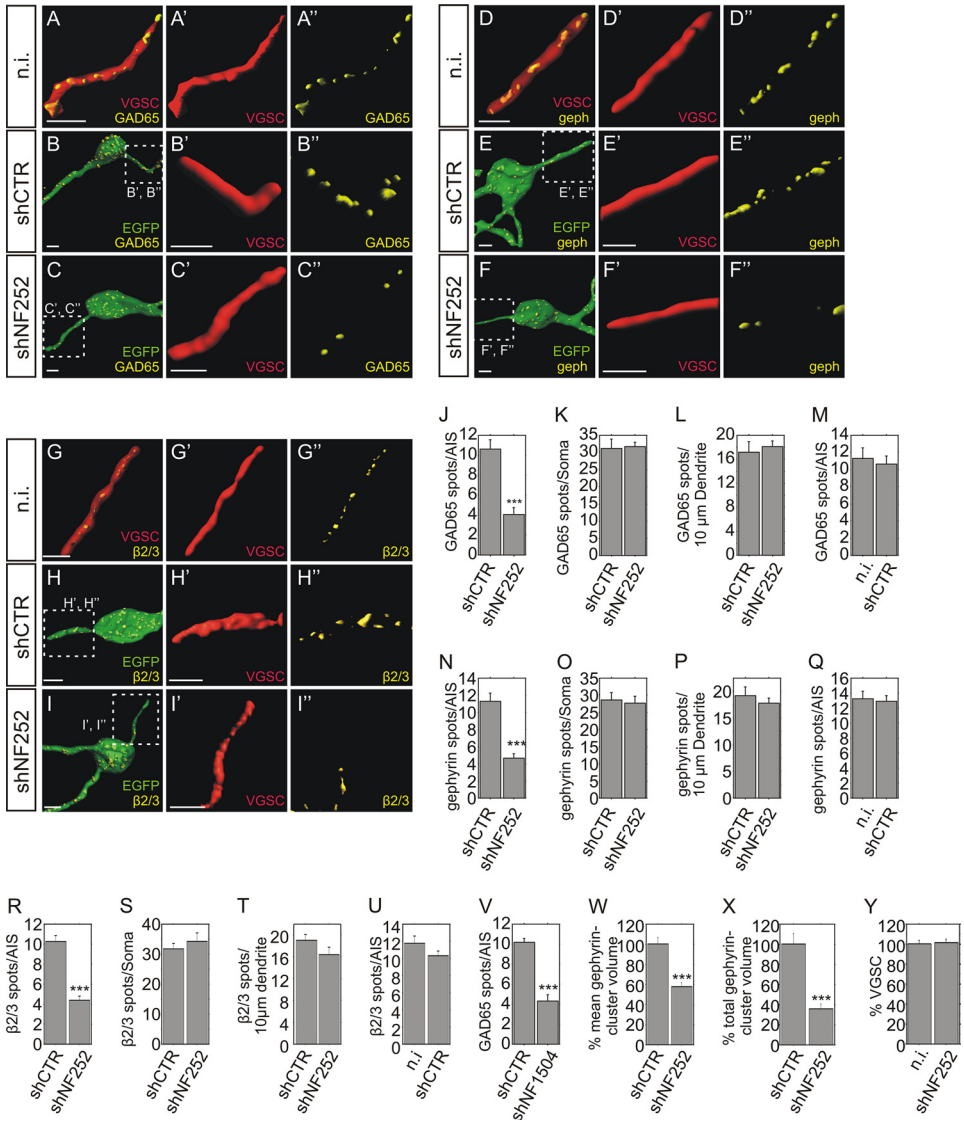

FIGURE 2. **GABAergic markers are reduced after suppression of neurofascin expression in adult rat hippocampal neurons.** Rendered images of granular cells of the dentate gyrus of adult rats were analyzed in uninfected (*n.i.*; *A*, *D*, and *G*), shCTR-infected (*B*, *E*, and *H*), or shNF252-infected (*C*, *F*, and *I*) tissue. The VGSC-positive AIS of infected *versus* uninfected neurons were discriminated by the presence or absence of lentivirally expressed EGFP (compare *A*, *D*, and *G* with *B*, *C*, *E*, *F*, *H*, and *I*, respectively). Presynaptic structures were detected by GAD65 staining (*A–C*) whereas postsynaptic components were visualized by gephyrin (*D–F*) as well as $GABA_AR$ subunit β2/3 staining (*G–I*). *Insets* in *B*, *C*, *E*, *F*, *H*, and *I* are enlarged in *B′*, *C′*, *E′*, *F′*, *H′*, *I′*, *B″*, *C″*, *E″*, *F″*, *H″*, and *I″*. *Scale bars*: 5 μm. *J–L*, quantification of GAD65-positive presynaptic terminals on AIS, somata, and dendritic fragments of control (shCTR)- and neurofascin-knockdown (shNF252)-infected neurons. *M*, quantification of GAD65-positive presynaptic terminals on AIS of uninfected (*n.i.*) and shCTR-infected neurons from the same animal. *N–P*, quantification of gephyrin-positive postsynaptic structures on AIS, somata, and dendritic fragments of control (shCTR)- and neurofascin-knockdown (shNF252)-infected neurons. *Q*, quantification of gephyrin-positive postsynaptic structures on AIS of uninfected and control-infected neurons from the same animal. *R–T*, quantification of $GABA_AR$ subunit β2/3-positive postsynaptic spots on AIS, somata, and dendritic fragments of control (shCTR)- and neurofascin-knockdown (shNF252)-infected neurons. *U*, quantification of $GABA_AR$ subunit β2/3-positive postsynaptic structures on AIS of uninfected and control-infected neurons from the same animal. *V*, quantification of GAD65-positive presynaptic terminals on the AIS of control neurons and neurons infected with a second independent neurofascin-knockdown viral vector (NF1504). *W*, quantification of the mean gephyrin cluster volume at the AIS. *X*, quantification of the total gephyrin cluster volume at the AIS. *Y*, quantification of VGSC expression on the AIS of neurofascin-knockdown infected and uninfected hippocampal granule cells from the same animal. ($n = 20$ for all groups; unpaired *t* test; ***, $p < 0.001$; *error bars* represent S.E.).

EGFP-gephyrin. Overexpression of the alternative neurofascin isoform NF186 was ineffective (Fig. 3*C*). Likewise, overexpression of neurofascin NF166 deletion mutants lacking either the intracellular or the extracellular domain (NF166-ED and NF-CD, respectively) did not increase gephyrin cluster size, indicating that full-length neurofascin is required for increasing gephyrin cluster size in primary neurons. Finally, EGFP-gephyrin colocalizes with endogenous γ2 subunits of $GABA_A$ receptors both in the presence and absence of neurofascin NF166 expression, indicating that EGFP-gephyrin is incorporated into endogenous postsynaptic protein complexes (Fig. 3*F*). In conclusion, these experiments suggest a role for NF166 in the control of gephyrin cluster size.

We further observed no impact of lentiviral shNF252-mediated knockdown of neurofascin on endogenous gephyrin clustering in hippocampal neurons (Fig. 3, *D* and *E*). The obvious difference in the *in vivo* experiments may be explained by the divergent expression pattern of neurofascin isoforms *in vitro*

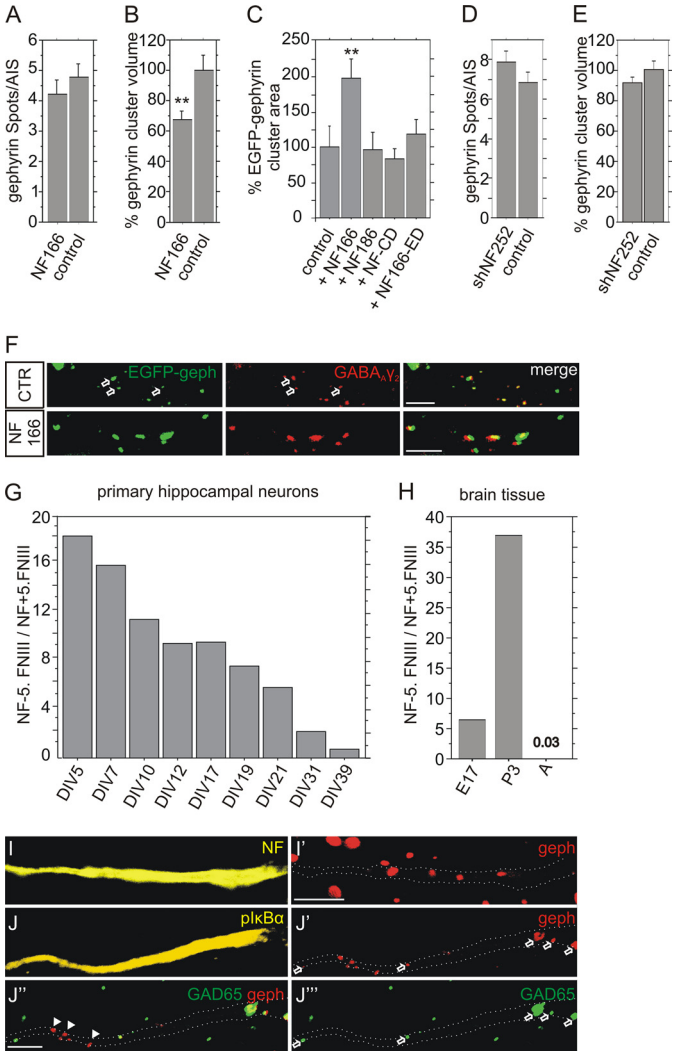

FIGURE 3. **Neurofascin controls gephyrin cluster size after transfection in cultured hippocampal neurons.** *A* and *B*, overexpression of NF166 after transfection and analysis of the number or volume of endogenous gephyrin clusters at the AIS, n>60, ANOVA; **, $p < 0.01$; *error bars* represent S.E. *C*, transfection of an EGFP-gephyrin expression vector in the absence (control) or presence of neurofascin NF166, NF186, or deletion mutants. The mean area of individual gephyrin cluster was determined at the cell surface; n>30, ANOVA; **, $p < 0.01$; *error bars* represent S.E. *D* and *E*, lentiviral expression of shNF252 in hippocampal neurons and analysis of the number or volume of endogenous gephyrin clusters at the AIS. For *D*: $n = 50$, ANOVA; *error bars* represent S.E. For *E*: n>350. *F*, colocalization of endogenous GABA$_A$R γ2 subunit with overexpressed EGFP-gephyrin in the absence (control) or presence of NF166. *G* and *H*, ratio of $NF_{-5.FNIII}/NF_{+5.FNIII}$ as measured by quantitative RT-PCR of cultured neurons at indicated DIVs or of brain tissue of embryonic day 17 (*E17*), postnatal day 3 (*P3*) or of the adult brain (*A*, $p > 90$), respectively. *I* and *I'*, colocalization of neurofascin-positive AIS with endogenous gephyrin as detected by immunostaining of cultured hippocampal neurons. Neurofascin-stained AIS (*I*, *yellow*) are represented in *I'* (gephyrin immunostaining, *red*) as *dotted lines*. *J–J'''*, triple fluorescence analysis of hippocampal neurons stained for the AIS marker pI$_K$Bα (*J*, *yellow*), postsynaptic gephyrin (*J'*, *red*) and presynaptic GAD65 (*J'''*, *green*). *J''*, merge of *J'* and *J'''*. pI$_K$Bα-stained AIS are indicated in *J'–J'''* as *dotted lines*. *Scale bar*: 5 μm.

(see above) as well as incomplete maturation of cultured hippocampal neurons. Therefore, we examined the maturation state of GABAergic synapses at the AIS of hippocampal neurons. As shown in Fig. 3, *I* and *J*, neurofascin and the AIS marker protein phospho-I$_K$Bα (25) are coexpressed at the AIS. However, a considerable number of postsynaptic gephyrin clusters on phospho-I$_K$Bα-labeled AIS (Fig. 3*J'*) were devoid of opposed GAD65-positive terminals (see *arrowheads* in Fig. 3, *J–J'''*). Consequently, cultured neurons showed only partial elaboration of pre- and postsynaptic elements at the AIS, indicating incomplete maturation. By contrast, essentially all gephyrin clusters colocalize with GABAergic terminals at the AIS of adult brain *in vivo* (Fig. 1*E*).

NF166 Regulates Gephyrin Cluster Size in Hippocampal Neurons via FGFR1 Signaling—Neurofascin is a member of a class of cell adhesion molecules including NCAM and L1 that are thought to act via FGFR1 signaling (17, 26, 27). We therefore investigated a possible role of FGFR1 signaling in gephyrin clustering at the AIS after cotransfection of hippocampal neurons with neurofascin, EGFP-gephyrin, and a dominant negative mutant of FGFR1 (dnFGFR1). Overexpression of dnFGFR1 reduced gephyrin cluster size in the presence of neurofascin NF166 to the level of controls lacking NF166 (Fig. 4*C*). The same outcome was found for the application of the specific FGFR1 inhibitor SU5402. However, both SU5402 and dnFGFR1 did not impair EGFP-gephyrin cluster size in control neurons in the absence of NF166 overexpression, indicating that FGFR1 signaling is not involved in basal gephyrin clustering, but may contribute to the neurofascin-dependent organization of gephyrin clustering.

Neurofascin Expression Enhances Gephyrin Clustering in HeLa Cells—To study the function of neurofascin in a further independent model we made use of non-neuronal cells as a tool to study gephyrin clustering (4, 28, 29). HeLa cells were transiently transfected with expression vectors for neurofascin, EGFP-gephyrin, and the neuronal RhoGEF collybistin that is essential for translocating gephyrin to submembrane microaggregates (4, 29). We chose a constitutively active collybistin variant ($CB2_{SH3-}$) because we wished to assess the impact of neurofascin on gephyrin clustering in the absence of neuroligin 2, which activates collybistin splice variants containing the *src* homology domain (4).

Expression of neurofascin isoform NF166 increased EGFP-gephyrin submembrane cluster size in the presence of collybistin compared with cells expressing other cell adhesion molecules such as NCAM, L1 or control transfected cells (Fig. 5, *A–C*). Quantitative immunofluorescence revealed a 70% increase in the average area of EGFP-gephyrin clusters compared with controls (Fig. 5*C*). Interestingly, the increase in cluster size is accompanied by a decrease in cluster number, suggesting fusion of gephyrin molecules into larger protein complexes (Fig. 5*F*). In addition, confocal analysis revealed that neurofascin is largely excluded from clustered EGFP-gephyrin in HeLa cells (Fig. 5*B''*). A NF166 deletion mutant lacking the intracellular domain of neurofascin did not increase gephyrin cluster size as observed in primary neurons. However, expression of NF186 or the neurofascin deletion mutant NF-CD lacking extracellular domains also induced gephyrin cluster size in a manner comparable to NF166 (Fig. 5*C*). Thus, the specificity for NF166 *versus* NF186 in the control of gephyrin clustering and the requirement of full-length neurofascin observed in primary neurons have been lost in the HeLa cell model.

As found in primary neurons, neurofascin-dependent gephyrin clustering in HeLa cells was abolished by coexpression of

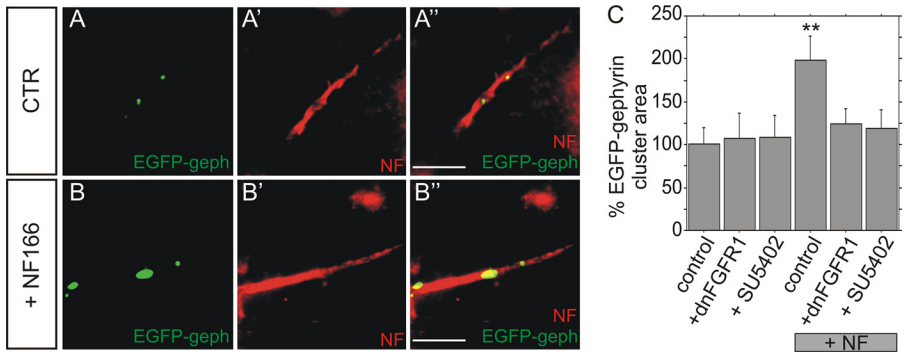

FIGURE 4. **Neurofascin-induced gephyrin clustering is impaired by the inhibition of FGFR signaling.** *A* and *B*, double fluorescence analysis of hippocampal neurons in the absence (*CTR*) or presence (*NF166*) of neurofascin NF166. Endogenous neurofascin is detected by a Cy3-labeled secondary antibody (*A′–A″* and *B′–B″*) to mark the AIS, whereas EGFP fluorescence was detected for the localization of EGFP-gephyrin. *Scale bars*: 5 μm. *C*, analysis of EGFP-gephyrin cluster areas on the AIS of hippocampal neurons in the absence or presence of NF166 (+*NF*) overexpression. Cells were either cotransfected with dnFGFR1 or exposed to the FGFR inhibitor SU5402. n>40 for all groups, ANOVA; **, $p < 0.01$; *error bars* represent S.E.

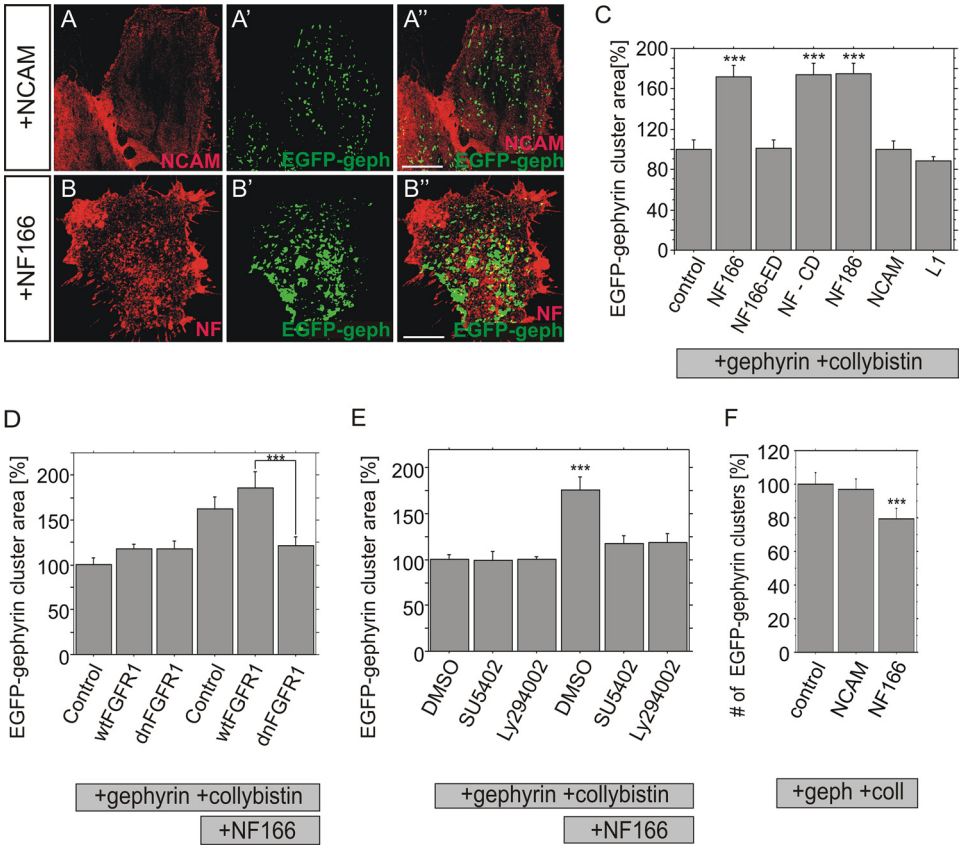

FIGURE 5. **Neurofascin regulates gephyrin cluster size in HeLa cells.** NCAM (*A–A″*) or neurofascin (*B–B″*) were coexpressed with EGFP-gephyrin and collybistin II ($CB2_{SH3-}$ isoform). Increased EGFP-gephyrin cluster size (*green*) was observed in the presence of neurofascin. NCAM/neurofascin immunofluorescence (*red*) is shown in *A* and *B* whereas EGFP-gephyrin in the same cell is indicated in *A′* and *B′*. Merged images are shown in *A″* and *B″*. *Scale bars*: 10 μm. *C*, quantification of the average area of individual gephyrin clusters in transfected HeLa cells as shown in *A* and *B* in the absence (control) or the presence of neurofascin NF166, NF186, NCAM, L1 as well as neurofascin mutants NF166-ED (cytosolic domain deleted) or NF-CD (extracellular domain removed). n>2500 for all groups. *D*, quantification of gephyrin cluster size after overexpression of neurofascin together with dnFGFR1 or wild-type FGF receptor1 (wtFGFR1). n>1400 for all groups. *E*, quantification of the average area of individual gephyrin clusters after overexpression of neurofascin, collybistin II, and EGFP-gephyrin as well as concomitant treatment with inhibitors specific for FGF receptor 1 (SU5402) or PI3K (LY294002). n>2500 for all groups. *F*, number of cell surface EGFP-gephyrin clusters per cell. n>40 for all groups, ANOVA; ***, $p < 0.001$; *error bars* represent S.E.

dn-FGFR1, but not of wild-type FGFR1 (Fig. 5*D*). This finding was further corroborated by the observation that both the specific FGFR inhibitor SU5402 and the inhibitor Ly94002 specific for the FGFR downstream component PI3K decrease neurofascin-dependent gephyrin clustering (Fig. 5*E*). In summary, these results imply that neurofascin-dependent gephyrin clustering may be controlled in HeLa cells by FGFR1 signaling principally as observed in primary neurons.

Neurofascin Modulates the Clustering of Inhibitory $GABA_A$ Receptors—We also assessed the possible impact of neurofascin on the clustering of $\alpha2\beta3\gamma2$ $GABA_A$Rs that reside on the AIS of hippocampal neurons (30). This was accomplished by express-

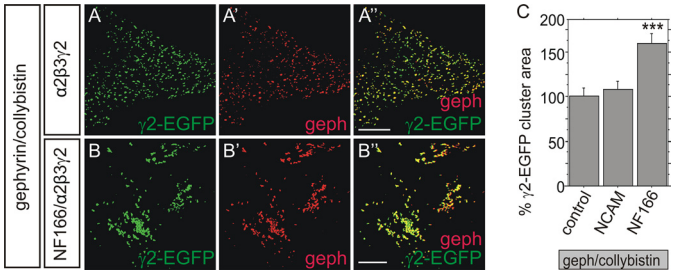

FIGURE 6. **Clustering of $\alpha_2\beta_3\gamma_2$ GABA$_A$ receptors is increased after overexpression of neurofascin.** Representative immunofluorescence images were taken from HeLa cells in the absence (*A–A″*) or presence (*B–B″*) of neurofascin expression. HeLa cells were cotransfected with gephyrin, collybistin II ($CB2_{SH3-}$), and $\alpha_2\beta_3\gamma_2$ GABA$_A$ receptors. The GABA$_A$R γ_2 subunit was fused to EGFP for visualization (*A* and *B*, *green*, γ2-EGFP), gephyrin was detected via immunocytochemistry (*A′* and *B′*, *red*). Merged image is shown in *A″* and *B″*. *Scale bars*: 10 μm. *C*, quantification of the mean size of individual GABA$_A$R subunit clusters in transfected HeLa cells as in *A* and *B* in a control situation (control) or after cotransfection of NCAM or neurofascin. n>1500 for all groups, ANOVA; ***, $p < 0.001$; *error bars* represent S.E.

ing EGFP-tagged γ2 with untagged α2/β3 subunits in combination with collybistin and gephyrin in HeLa cells. As shown in Fig. 6*A*, gephyrin detected by immunocytochemistry perfectly colocalizes with γ2-EGFP, indicating that GABA$_A$Rs were assembled correctly and associated with submembrane gephyrin. In the presence of neurofascin (Fig. 6*B*), colocalization of gephyrin with γ2-EGFP was retained. However, GABA$_A$R clusters appeared to be fused into larger aggregates. Accordingly, quantification of the average area of individual γ2-EGFP clusters demonstrated that neurofascin expression results in increased average γ2-EGFP cluster size (Fig. 6*C*). By contrast, γ2-EGFP cluster areas remained unchanged after overexpression of NCAM.

DISCUSSION

This study demonstrates that neurofascin knockdown impairs both gephyrin and GABA$_A$R clustering as well as the stability of GABAergic input at the AIS *in vivo*. Likewise, neurofascin appeared to be involved both in the regulation of the number and the size of gephyrin clusters. Moreover, gephyrin cluster size was also controlled by neurofascin in two distinct *in vitro* model systems, in hippocampal neurons and in HeLa cells, presumably dependent on FGFR1 signaling.

In the hippocampus, the AIS of dentate gyrus granular cells is targeted by axo-axonic terminals almost exclusively derived from chandelier neurons (6). The site of inhibitory input is thought to be strategic, because these terminals control the activity of principal neurons. Our results indicate that neurofascin may play an important role in the stabilization of axo-axonic input at the AIS of granular cells *in vivo*.

To get more insight into molecular mechanisms involved, our analysis relied on the use of two *in vitro* models including hippocampal neurons and a HeLa cell model. In a similar approach, non-neuronal cells such as HEK-293 cells were previously used to dissect mechanisms of gephyrin clustering (4, 28, 29). However, experimental limitations of the HeLa cell model need to be considered because tumor cells may make use of signaling pathways presumably different from those found in neurons. On the other hand, one of the key findings that FGFR1 signaling may contribute to neurofascin NF166-dependent gephyrin clustering was reproduced both in hippocampal neurons and in HeLa cells. The results also need to be cautiously interpreted because relevant neuronal factors may be missing in this model system. For instance, both NF166 and NF186 induced gephyrin clustering in HeLa cells, equally. This was not observed in cultured neurons where only NF166 was effective.

Neurofascin knockdown reduces clustering of gephyrin and GABA$_A$ receptors. The finding raises the question which of these pre- and postsynaptic components is primarily addressed by neurofascin. Gephyrin, a scaffolding component of GABA$_A$Rs, is associated with gephyrin and collybistin (29, 31). Several reports suggest that basal assembly of this protein complex is independent of neurofascin expression (29, 31, 32). Therefore, neurofascin may be more implicated in functions of gephyrin cluster stabilization or size control, specifically at the AIS.

We also observed reduction of GAD65-positive presynaptic terminals after neurofascin knockdown *in vivo*. As a cell surface protein expressed in postsynaptic cells, neurofascin may trigger presynaptic stabilization via transsynaptic adhesion to presynaptic ligands very similar to *e.g.* neurexin-neuroligin or ephrinB-EphB interactions (33–36). Interference with neurofascin expression may therefore release synaptic contact. However, neurofascin is evenly distributed at the AIS of postsynaptic cells and does not display clustered expression at the subsynaptic membrane as shown for the other cell adhesion molecules, which argues against a specific role in transsynaptic adhesion. Alternatively, neurofascin may indirectly control presynaptic stabilization via stabilization of the GABA$_A$R-gephyrin cluster complex. In case of neurofascin knockdown, disturbed expression and localization of GABA$_A$Rs per se may be sufficient to destabilize presynaptic input (37). Hence, transsynaptic adhesion may not represent an absolute requirement for neurofascin-dependent presynaptic stabilization.

Considering mechanistic possibilities of neurofascin-dependent gephyrin clustering, neurofascin may be integrated into gephyrin-associated protein complexes at subsynaptic membranes. So far, we could not provide evidence for a direct interaction of neurofascin with gephyrin because neither yeast two-hybrid nor immunoprecipitation assays showed any direct or indirect interaction.[5] In the HeLa cell model, neurofascin appeared to be excluded from submembrane gephyrin clusters. The exclusion of neurofascin from sites of submembrane gephyrin clusters may be explained by steric hindrance. Interaction of membrane-associated gephyrin with cytosolic interaction partners including microtubules may displace the cytosolic domain of neurofascin (38). Alternatively, the link between neurofascin and gephyrin clustering may rely on FGFR1 signaling which is required for gephyrin clustering both in hippocampal neurons and in HeLa cells. Neurofascin is able to interact with FGFR1 via intra- as well as extracellular domains, and neurofascin-dependent FGFR1 signaling is involved in the induction of neurite outgrowth upon homophilic interaction in embryonic neurons (17). Association with FGFR1 signaling and control of synaptic organization are prop-

[5] M. Kriebel, J. Metzger, S. Trinks, D. Chugh, R. J. Harvey, K. Harvey, and H. Volkmer, unpublished data.

erties shared with other cell adhesion molecules *e.g.* NCAM (17, 26, 27). NCAM regulates the formation or stabilization of excitatory synapses on dendrites (39). Altogether, the findings raise the interesting possibility that FGFR1 signaling is involved both in inhibitory and excitatory synapse stabilization via interaction with cell adhesion molecules.

Our results also suggest different roles of neurofascin isoforms in gephyrin clustering because NF186 did not increase gephyrin cluster size in contrast to NF166. NF186 is expressed predominantly in adult brain, suggesting a possible role for the stabilization of gephyrin clusters. Accordingly, NF186 was recently defined as a central element for the anchoring of AIS components (40). On the other hand, our experiments suggest an additional role for neurofascin in the dynamics of gephyrin clustering. The observation that NF166 modulated gephyrin cluster size at the AIS of hippocampal neurons is in line with this assumption. In a previous report, low density cultures of hippocampal neurons served as a model for the *de novo* formation of gephyrin clusters at the soma and the axon hillock (18). These immature neurons were devoid of completely differentiated AIS and expressed NF166, exclusively. Heterochronous expression of NF186 reduced the number of gephyrin punctae at the soma and therefore interfered with *de novo* gephyrin cluster formation. Presumably, NF186 competed for interaction partners of endogenous NF166 which were required for the formation of gephyrin clusters. By contrast, NF166 overexpression in the more mature neurons shown here modulated the size and not the number of preexisting gephyrin clusters at the AIS. In conclusion, different hippocampal model systems appear to reveal distinct neurofascin functions.

NF186 and NF166 represent two of a variety of neurofascin isoforms expressed in brain. Differences in the expression of extracellular domains account for selective interactions with extracellular ligands (19, 24, 41). Hence, the different functions of NF186 and NF166 may rely on selective recognition of extracellular ligand proteins. Different extracellular candidate interaction partners have been identified, including cell surface proteins axonin-1, F11/contactin, and NrCAM as well as with the component of the extracellular matrix tenascin-R (19, 42, 43). Of particular interest for an involvement in gephyrin clustering is NrCAM which is specifically coexpressed with neurofascin at the AIS of Purkinje neurons (44).

It was a surprising observation that NF166 decreased endogenous gephyrin cluster size whereas increased cluster size was measured in the presence of overexpressed EGFP-gephyrin. Control transfections as well as the finding that EGFP-gephyrin was incorporated into endogenous gephyrin clusters argue against overexpression artifacts as a possible reason. Furthermore, sensitivity of EGFP-gephyrin clustering to inhibition of FGFR1 signaling indicated further specificity for neurofascin-dependent mechanism. One explanation may be put forth by the dual properties of hippocampal neurons under study. These neurons displayed features of mature stabilized structures as exemplified by "adult" NF186 expression and completed organization of AIS components including expression of gephyrin clusters. However, coexpression of "embryonic" NF166 as well as the only partial elaboration of presynaptic terminals implied aspects of incomplete maturation. Gephyrin clusters located at the AIS of hippocampal neurons may require NF186 for stabilization. If neurons were overloaded with NF166, NF166 could compete with endogenous NF186 for binding to factors involved in gephyrin cluster stabilization. Consequently, endogenous gephyrin clusters may become destabilized. By contrast, simultaneous overexpression of EGFP-gephyrin might provide a pool of gephyrin amenable to NF166-mediated integration into preformed gephyrin clusters. In this case the destabilizing properties of NF166 are counteracted by increased gephyrin cluster assembly resulting in net increased gephyrin cluster size.

A picture of the organization of inhibitory synapses on principal neurons now becomes clearer. Neuroligin 2 is a major player to assemble dendritic and perisomatic inhibitory synapses (4, 45). Neurofascin represents a further cell surface molecule implicated in the organization of GABAergic synapses at the AIS. A function of neurofascin for synapse organization at dendrites or in the perisomatic compartment is less probable. Both the restricted expression of neurofascin at the AIS and the finding that neurofascin knockdown does not impair GABAergic innervation outside of the AIS argue against this possibility. Whether neuroligin 2 is also involved in gephyrin clustering at the AIS, remains elusive.

Acknowledgments—We thank Ursula Härle for technical assistance and Annyesha Mohanti for help constructing $GABA_A$ receptor expression plasmids, G. O'Sullivan for the EGFP-gephyrin, and Pavel Osten for the CamKII promoter constructs.

REFERENCES

1. Gerrow, K., and El-Husseini, A. (2006) *Front. Biosci.* **11,** 2400–2419
2. Chih, B., Engelman, H., and Scheiffele, P. (2005) *Science* **307,** 1324–1328
3. Graf, E. R., Zhang, X., Jin, S. X., Linhoff, M. W., and Craig, A. M. (2004) *Cell* **119,** 1013–1026
4. Poulopoulos, A., Aramuni, G., Meyer, G., Soykan, T., Hoon, M., Papadopoulos, T., Zhang, M., Paarmann, I., Fuchs, C., Harvey, K., Jedlicka, P., Schwarzacher, S. W., Betz, H., Harvey, R. J., Brose, N., Zhang, W., and Varoqueaux, F. (2009) *Neuron* **63,** 628–642
5. Somogyi, P., Smith, A. D., Nunzi, M. G., Gorio, A., Takagi, H., and Wu, J. Y. (1983) *J. Neurosci.* **3,** 1450–1468
6. Howard, A., Tamas, G., and Soltesz, I. (2005) *Trends Neurosci.* **28,** 310–316
7. Woodruff, A. R., Anderson, S. A., and Yuste, R. (2010) *Front. Neurosci.* **4,** 201
8. Lewis, D. A. (2011) *Dev. Neurobiol.* **71,** 118–127
9. Ogawa, Y., and Rasband, M. N. (2008) *Curr. Opin. Neurobiol.* **18,** 307–313
10. Kordeli, E., Lambert, S., and Bennett, V. (1995) *J. Biol. Chem.* **270,** 2352–2359
11. Berghs, S., Aggujaro, D., Dirkx, R., Jr., Maksimova, E., Stabach, P., Hermel, J. M., Zhang, J. P., Philbrick, W., Slepnev, V., Ort, T., and Solimena, M. (2000) *J. Cell Biol.* **151,** 985–1002
12. Jenkins, S. M., and Bennett, V. (2001) *J. Cell Biol.* **155,** 739–746
13. Hassel, B., Rathjen, F. G., and Volkmer, H. (1997) *J. Biol. Chem.* **272,** 28742–28749
14. Hedstrom, K. L., Xu, X., Ogawa, Y., Frischknecht, R., Seidenbecher, C. I., Shrager, P., and Rasband, M. N. (2007) *J. Cell Biol.* **178,** 875–886
15. Ratcliffe, C. F., Westenbroek, R. E., Curtis, R., and Catterall, W. A. (2001) *J. Cell Biol.* **154,** 427–434
16. Sherman, D. L., Tait, S., Melrose, S., Johnson, R., Zonta, B., Court, F. A., Macklin, W. B., Meek, S., Smith, A. J., Cottrell, D. F., and Brophy, P. J. (2005) *Neuron* **48,** 737–742
17. Kirschbaum, K., Kriebel, M., Kranz, E. U., Pötz, O., and Volkmer, H. (2009)

J. Biol. Chem. **284,** 28533–28542
18. Burkarth, N., Kriebel, M., Kranz, E. U., and Volkmer, H. (2007) *Mol. Cell. Neurosci.* **36,** 59–70
19. Pruss, T., Kranz, E. U., Niere, M., and Volkmer, H. (2006) *Mol. Cell. Neurosci.* **31,** 354–365
20. Freund, T. F., and Buzsáki, G. (1996) *Hippocampus* **6,** 347–470
21. Hardwick, C., French, S. J., Southam, E., and Totterdell, S. (2005) *Brain Res.* **1031,** 238–244
22. McEwen, D. P., and Isom, L. L. (2004) *J. Biol. Chem.* **279,** 52744–52752
23. Dzhashiashvili, Y., Zhang, Y., Galinska, J., Lam, I., Grumet, M., and Salzer, J. L. (2007) *J. Cell Biol.* **177,** 857–870
24. Koticha, D., Babiarz, J., Kane-Goldsmith, N., Jacob, J., Raju, K., and Grumet, M. (2005) *Mol. Cell. Neurosci.* **30,** 137–148
25. Schultz, C., König, H. G., Del Turco, D., Politi, C., Eckert, G. P., Ghebremedhin, E., Prehn, J. H., Kögel, D., and Deller, T. (2006) *Mol. Cell. Neurosci.* **33,** 68–80
26. Ditlevsen, D. K., Povlsen, G. K., Berezin, V., and Bock, E. (2008) *J. Neurosci. Res.* **86,** 727–743
27. Maness, P. F., and Schachner, M. (2007) *Nat. Neurosci.* **10,** 19–26
28. Harvey, K., Duguid, I. C., Alldred, M. J., Beatty, S. E., Ward, H., Keep, N. H., Lingenfelter, S. E., Pearce, B. R., Lundgren, J., Owen, M. J., Smart, T. G., Lüscher, B., Rees, M. I., and Harvey, R. J. (2004) *J. Neurosci.* **24,** 5816–5826
29. Saiepour, L., Fuchs, C., Patrizi, A., Sassoè-Pognetto, M., Harvey, R. J., and Harvey, K. (2010) *J. Biol. Chem.* **285,** 29623–29631
30. Nusser, Z., Sieghart, W., Benke, D., Fritschy, J. M., and Somogyi, P. (1996) *Proc. Natl. Acad. Sci. U.S.A.* **93,** 11939–11944
31. Tretter, V., Jacob, T. C., Mukherjee, J., Fritschy, J. M., Pangalos, M. N., and Moss, S. J. (2008) *J. Neurosci.* **28,** 1356–1365
32. Jacob, T. C., Moss, S. J., and Jurd, R. (2008) *Nat. Rev. Neurosci.* **9,** 331–343
33. Song, J. Y., Ichtchenko, K., Südhof, T. C., and Brose, N. (1999) *Proc. Natl. Acad. Sci. U.S.A.* **96,** 1100–1105
34. Dalva, M. B., Takasu, M. A., Lin, M. Z., Shamah, S. M., Hu, L., Gale, N. W., and Greenberg, M. E. (2000) *Cell* **103,** 945–956
35. Varoqueaux, F., Jamain, S., and Brose, N. (2004) *Eur. J. Cell Biol.* **83,** 449–456
36. Craig, A. M., Graf, E. R., and Linhoff, M. W. (2006) *Trends Neurosci.* **29,** 8–20
37. Li, R. W., Yu, W., Christie, S., Miralles, C. P., Bai, J., Loturco, J. J., and De Blas, A. L. (2005) *J. Neurochem.* **95,** 756–770
38. Fritschy, J. M., Harvey, R. J., and Schwarz, G. (2008) *Trends Neurosci.* **31,** 257–264
39. Cambon, K., Hansen, S. M., Venero, C., Herrero, A. I., Skibo, G., Berezin, V., Bock, E., and Sandi, C. (2004) *J. Neurosci.* **24,** 4197–4204
40. Zonta, B., Desmazieres, A., Rinaldi, A., Tait, S., Sherman, D. L., Nolan, M. F., and Brophy, P. J. (2011) *Neuron* **69,** 945–956
41. Basak, S., Raju, K., Babiarz, J., Kane-Goldsmith, N., Koticha, D., and Grumet, M. (2007) *Dev. Biol.* **311,** 408–422
42. Volkmer, H., Leuschner, R., Zacharias, U., and Rathjen, F. G. (1996) *J. Cell Biol.* **135,** 1059–1069
43. Volkmer, H., Zacharias, U., Nörenberg, U., and Rathjen, F. G. (1998) *J. Cell Biol.* **142,** 1083–1093
44. Davis, J. Q., Lambert, S., and Bennett, V. (1996) *J. Cell Biol.* **135,** 1355–1367
45. Chubykin, A. A., Atasoy, D., Etherton, M. R., Brose, N., Kavalali, E. T., Gibson, J. R., and Südhof, T. C. (2007) *Neuron* **54,** 919–931